Free Radical Biology and Medicine 53 (2012) 2146–2158

Contents lists available at SciVerse ScienceDirect

Free Radical Biology and Medicine

journal homepage: www.elsevier.com/locate/freeradbiomed

Methods in Free Radical Biology and Medicine

A multilevel analytical approach for detection and visualization of intracellular NO production and nitrosation events using diaminofluoresceins

Miriam M. Cortese-Krott [a,*], Ana Rodriguez-Mateos [b], Gunter G. C. Kuhnle [b], Geoff Brown [c], Martin Feelisch [d], Malte Kelm [a]

[a] Cardiovascular Research Laboratory, Department of Cardiology, Pneumology, and Angiology, Medical Faculty, Heinrich Heine University, Düsseldorf 40225, Germany
[b] Department of Food and Nutritional Sciences, Reading, UK
[c] Department of Chemistry, University of Reading, Reading, UK
[d] Clinical & Experimental Sciences, Faculty of Medicine, University of Southampton, Southampton General Hospital, Southampton, UK

ARTICLE INFO

Article history:
Received 4 July 2012
Received in revised form
5 September 2012
Accepted 12 September 2012
Available online 28 September 2012

Keywords:
Nitric oxide
Fluorescence imaging
DAF-FM
DAF-2
Nitrosation
Red blood cells
Free radicals

ABSTRACT

Diaminofluoresceins are widely used probes for detection and intracellular localization of NO formation in cultured/isolated cells and intact tissues. The fluorinated derivative 4-amino-5-methylamino-2′,7′-difluorofluorescein (DAF-FM) has gained increasing popularity in recent years because of its improved NO sensitivity, pH stability, and resistance to photobleaching compared to the first-generation compound, DAF-2. Detection of NO production by either reagent relies on conversion of the parent compound into a fluorescent triazole, DAF-FM-T and DAF-2-T, respectively. Although this reaction is specific for NO and/or reactive nitrosating species, it is also affected by the presence of oxidants/antioxidants. Moreover, the reaction with other molecules can lead to the formation of fluorescent products other than the expected triazole. Thus additional controls and structural confirmation of the reaction products are essential. Using human red blood cells as an exemplary cellular system we here describe robust protocols for the analysis of intracellular DAF-FM-T formation using an array of fluorescence-based methods (laser-scanning fluorescence microscopy, flow cytometry, and fluorimetry) and analytical separation techniques (reversed-phase HPLC and LC-MS/MS). When used in combination, these assays afford unequivocal identification of the fluorescent signal as being derived from NO and are applicable to most other cellular systems without or with only minor modifications.

Introduction

Nitric oxide (NO; nitrogen monoxide) is a key signaling molecule that fulfills crucial regulatory functions in physiology and pathophysiology [1]. It is produced by virtually every cell throughout all organ systems via various enzymatic and nonenzymatic routes, and its chemistry and biochemistry are tightly linked to its biological function [2,3]. The reactivity of NO in biological systems depends on the rate of formation, the resultant local concentration, the localization of the NO source, the biological targets and reactants in its vicinity, as well as the rate of diffusion within the cell or tissue [2]. In addition to the direct actions of locally formed NO, its tonic production gives rise to the formation of even longer-lived adducts and metabolites, which can act as transport and storage forms of NO.

The measurement of NO and its metabolites in complex biological matrices is notoriously difficult and technically demanding because of the relatively low concentrations of NO and its complex interaction with various other biological constituents [4–9]. Methods for the detection of intracellular NO production include (1) chemiluminescence techniques using the reaction of NO with ozone (gas phase) [4–9] or with molecules such as lucigenin and luminol/H_2O_2 (liquid phase) [10]; (2) fluorimetry using fluorescent NO-specific probes [11–15]; (3) spectrophotometry monitoring either the formation of NO–hemoglobin or the co-oxidation reaction with oxyhemoglobin to form methemoglobin and nitrate [16]; (4) EPR spectrometry using hemoglobin, nitronyl nitroxides, and iron–dithiocarbamate complexes as spin traps [17,18]; (5) electrochemical methods using (micro)electrodes specific to NO [19]; and, theoretically, (6) gas chromatography and mass spectrometry (although detection limits achieved may prevent its direct detection in most cases). Other indirect assays include spectrophotometric, fluorimetric, or radiometric assays measuring the rather more stable NO metabolites nitrite and nitrate or the by-product of L-arginine oxidation by nitric oxide synthases, L-citrulline [4]. All these methods have a distinct specificity, sensitivity, reproducibility, and technical demand/feasibility.

* Corresponding author. Fax: +0211 8115493.
E-mail address: miriam.cortese@uni-duesseldorf.de (M.M. Cortese-Krott).

0891-5849/$ - see front matter © 2012 Elsevier Inc. All rights reserved.
http://dx.doi.org/10.1016/j.freeradbiomed.2012.09.008

Despite all the limitations and pitfalls [20,21] the use of fluorescent probes to detect the formation of reactive oxygen and nitrogen species in cells and tissues has strongly contributed to the development of research in the field of free radical biology and medicine. In addition to the qualitative confirmation of free radical production in various experimental models, in some cases these reagents have allowed useful insights into their subcellular compartmentalization. Moreover, fluorescent probes are relatively cheap and signals can be detected by standard bench equipment such as fluorimeters, flow cytometers, and fluorescence microscopes. The experimental setup (including the appropriate controls) and the analytical methods chosen to detect the formation of fluorescent products ought to be carefully evaluated, because these molecules are seemingly easy *to use*, yet not necessarily easy *to apply* [20,21]. This is particularly true for 4,5-diaminofluorescein (DAF-2) and its derivatives (DAFs), originally synthesized by Nagano and colleagues [11,12]. These compounds have become the most popular and widely used fluorescent probes for the measurement of NO production in mammalian cells [15] and tissues [12,22], as well as in invertebrates and plants [12,23]. NO-dependent fluorescent product formation in cells and tissues has been mainly evaluated using fluorescence microscopy, flow cytometry, and fluorimetry [12,15,22], but the specificity of this approach has been questioned repeatedly [20,24,25]. In fact, these techniques are not able to distinguish the NO-specific fluorescent signal produced by the triazole derivates from nonspecific fluorescent products formed by reaction with other biological cell constituents within cells [12,22,26–28]. Although additional controls have been included by some investigators to exclude that changes in, e.g., ascorbate may have contributed to the measured changes in DAF-related fluorescence, not all possibilities for false positives may be known to date. Other uncertainties relate to the cellular redox status, which may also affect the intensity of the fluorescent signal that is observed, together with a high background due to preferential accumulation of DAFs within certain compartments and autofluorescence of cells and tissues [22]. This may make it difficult to detect basal NO production and, in some cases, prevent investigators from picking up a signal altogether. Most of these problems can be tackled by appropriate combination of techniques, in particular those that provide independent structural confirmation of the identity of reaction products. To this end, we here provide a multilevel analytical approach that combines fluorescence-based techniques (confocal laser scanning "live" cell microscopy, flow cytometry, and fluorimetry) with analytical separation techniques (high-performance liquid chromatography (HPLC) and LC coupled with tandem mass spectrometry (LC-MS/MS)) applicable to the detection of NO formation in cells. Combining single-cell analysis techniques such as flow cytometry and microscopy with liquid chromatography and mass spectrometry allows 4-amino-5-methylamino-2′,7′-difluorofluorescein (DAF-FM) (and related probes) to be used for unequivocal identification of NO formation and visualization of its production in cells and tissues.

Principles

DAF-FM is a fluorinated DAF-2 derivative with improved NO sensitivity, pH stability, and resistance to photobleaching [13].

For NO imaging with DAFs, cells are typically loaded with the respective diacetate derivative (e.g., DAF-FM-DA), which is cleaved by intracellular esterases to form the negatively charged parent compound, e.g., DAF-FM (Fig. 1). The latter cannot cross the cell membrane and thus accumulates inside the cells. In the presence of NO and oxygen a highly fluorescent triazole (DAF-FM-T) is formed. An increased fluorescence activity compared to the background can be detected by using an appropriate fluorescence detector.

DAFs are the most frequently used and best investigated NO imaging probes [25,29]. However, it is important to point out that these probes do not directly react with NO. The precise reaction chemistry and the mechanisms leading to triazole formation inside cells are still unknown. Two different mechanisms have been proposed, which are summarized in Fig. 1. Initially, Nagano and colleagues proposed that one of the vicinal amino groups of the DAFs interacts with reactive nitrosating species derived from the reaction of NO with O_2, such as N_2O_3 [15] or nitrous acid [14], to form an intermediary *N*-nitrosamine that—after intramolecular reaction with the adjacent amino group—is subsequently converted to the highly fluorescent triazole derivative, DAF-2-T or DAF-FM-T [25]. Later, Wardman pointed out that N_2O_3 is not likely to be formed efficiently in aqueous biological environments, except in lipid membranes [20]. He argued that in the cytosol, formation of N_2O_3 may not be necessary, as the formation of the

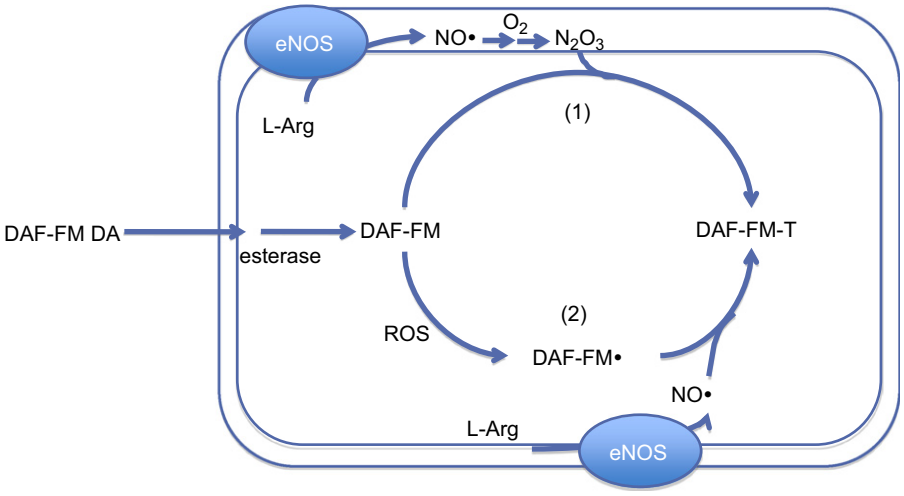

Fig. 1. Possible mechanisms of intracellular DAF-FM nitrosation within a cell having a source of NO. Endothelial NO synthase (eNOS) was chosen here simply as an example of an intracellular NO source; alternative sources of NO may originate from nitrite reduction and preformed storage forms of NO (not shown here for sake of simplicity). DAF-FM diacetate (DAF-FM-DA) diffuses into cells, where esterases hydrolyze the diacetate residues thereby trapping DAF-FM within the intracellular space. Here, DAF-FM reacts with NO (or derived molecules) to form the highly fluorescent corresponding triazole (DAF-FM-T). Two mechanisms have been proposed: (1) nitrosating species (such as dinitrogen trioxide, N_2O_3) formed by reaction of NO with oxygen, which are preferentially formed within the membrane, nitrosate DAF-FM to yield DAF-FM-T. (2) Alternatively, DAF-FM may be oxidized by reactive oxygen species (ROS) produced within the cells to a radical intermediate (DAF-FM$^{\bullet}$) that reacts directly with NO.

fluorescent triazole may occur—in analogy with lucigenin and luminol—in two stages, comprising a one-electron oxidation step to an anilinyl radical that subsequently reacts with NO in a radical–radical reaction [20]. This implies that DAF-2 derivatives after activation may detect both NO and N_2O_3, but also that these probes are susceptible to interference toward any reagent that serves to modify the steady-state concentration of the intermediate radical, including (1) oxidants, increasing its formation, and (2) antioxidants, potentially decreasing its formation (or reducing the oxidized probe) [20]. Indeed, Jourd'heuil observed an increase in the NO-dependent fluorescence signal of DAF-2 in the presence of oxidants [28]. Because high concentrations of antioxidants present in cells are able to scavenge nitrosating intermediates and/or reduce the oxidized probe, some of us argued that DAF-2 derivatives must be present at high, millimolar concentrations to allow detection of nitrosative chemistry inside cells [22].

An important aspect of consideration is the choice of method for measuring the formation of the fluorescent triazole. Methods that merely detect changes in fluorescence intensity, including fluorimetry, microscopy, and flow cytometry, cannot distinguish between specific (both NO- and DAF-dependent) and nonspecific (DAF-dependent but NO-independent) fluorescence signals. The latter could also be derived by formation of fluorescent adducts of DAFs with ascorbate and dehydroascorbate [27] or reaction with $HgCl_2$, as reported [22]. Although principally producing comparable results, these assays differ somewhat in selectivity; a side-by-side comparison of fluorescence-based techniques, as presented here later on, offers valuable insight into technique-specific assay characteristics. On the other hand, chromatographic separation techniques with fluorescence detection allow positive identification of the reaction products formed from DAFs inside cells.

All protocols presented in this paper have been optimized for one of the most challenging of biological targets, the human red blood cell (RBC). This contains not only high levels of low-molecular-weight antioxidants, such as glutathione and ascorbate, but also an abundance of hemoglobin, which have the ability to interfere with DAF-based detection by trapping NO, reacting with reactive nitrogen oxide species; affect DAF radical formation; and affect fluorescence quenching. In most cases, these assays can be applied without further change to other cellular systems.

Materials

(1) 4-Amino-5-methylamino-2′,7′-difluorofluorescein diacetate, Invitrogen (Karlsruhe, Germany), Cat. No. D-23844;
(2) 4-Amino-5-methylamino-2′,7′-difluorofluorescein, authentic standard, HPLC-grade, Sigma–Aldrich (Poole, UK), Cat. No. D1821-1 MG;
(3) BD-Falcon centrifuge and test tube, 50 ml, BD Bioscience (Heidelberg, Germany), Cat. No. 352098;
(4) BD-Falcon centrifuge and test tube, 5 ml, BD Bioscience, Cat. No. 352003;
(5) Cysteine hydrochloride (Cys–HCl), Sigma–Aldrich, Cat. No. C1276-10G;
(6) Eppendorf tubes, 1.5 ml, Axygen, Fisher Scientific, Cat. No. MTC-150-C;
(7) Eppendorf Safe-Lock microcentrifuge tubes, VWR International GmbH (Darmstadt, Germany), Cat. No. CA21008-960;
(8) Formic acid, HPLC grade, Fisher Scientific (Loughborough, UK), Cat. No. F/1900/PB17; acetonitrile, HPLC grade, Fisher Scientific, Cat. No. A/0626/17;
(9) HPLC vials from Chromacol, Fisher Scientific, Cat. No. VGA-100–145F;
(10) Hydrochloric acid (HCl), 5 M, Fisher Scientific, Cat. No. M/4056/17; sodium hydroxide (NaOH), Fisher Scientific, Cat. No. S/4920/53;
(11) Luna 3C18(2) 100 A guard cartridges, Phenomenex (Torrance, CA, USA), Cat. No. AJ0-4287;
(12) Luna C18(2) column (4.6 μm × 250 mm; 5 μm particle size), Phenomenex, Cat. No. 00F-4251-E0;
(13) C18(2) column (50 mm × 2.1 mm), Phenomenex, Cat. No. 00F-4251-E0;
(14) Methanol, HPLC grade, Fisher Scientific, Cat. No. M/4056/17;
(15) Sodium nitrite, pro analysis, ACS grade, Sigma–Aldrich, 31443-100 G;
(16) Phosphate-buffered solution (PBS), PAA Laboratories GmbH (Cölbe, Germany), Cat. No. H15-002;
(17) Sphero Rainbow calibration particles (six peaks), 6.0–6.4 μm, BD Bioscience, Cat. No. 556288;
(18) Trifluoroacetic acid, HPLC grade, Fisher Scientific, Cat. No. T/3258/PB05;
(19) Water, HPLC grade, Fisher Scientific, Cat. No. W/0106/17.

Instrumentation

(1) Analytical balance (sensitive to 0.1 mg);
(2) Pipettes;
(3) Water bath with shaking function or incubator/shaker for Eppendorf tubes;
(4) Centrifuge for 15- to 50-ml tubes and benchtop centrifuge, Rotina 38 R and Mikro 200 R, Hettich Lab Technology (Tuttlingen, Germany);
(5) Fluorimeter, FLUOstar Optima, equipped with fluorescence filters for excitation 485 nm and emission 520 nm, BMG Labtech (Offenburg, Germany);
(6) Flow cytometer, FACS Canto II; flow cytometric data were collected using the DIVA 5.0 software package and analyzed using FlowJo version 7.5.5 (TreeStar, Ashland, OR, USA);
(7) Laser-scanning microscope, Zeiss LSM 510 confocal, Carl Zeiss Jena GmbH (Jena, Germany), equipped with a Zeiss Plan Neofluar 63 × /1.3 oil DIC objective, 488 nm argon laser, and UV/488/543/633 nm beam splitter; fluorescence was recorded using a 540–30 nm bandpass filter, and micrographs were taken at 37 °C in a thermostated observation chamber;
(8) Agilent 1100 Series HPLC system, Agilent Technologies (Palo Alto, CA, USA), equipped with a quaternary pump (G1211A), an online vacuum degasser (G1379A), a thermostated autosampler (G1329A, G1330B), a thermostated column compartment (G1316A), a diode array detector (G1315B), and a fluorescence detector (G1321A);
(9) Mass spectrometer, Agilent 6400 triple–quadrupole LC-MS/MS instrument, Agilent Technologies, operated in positive-ion mode;
(10) Mass spectrometer, LTQ OrbiTrap, Thermo Fisher Scientific (Bremen, Germany);
(11) NMR spectrometer, 700 MHz on a Bruker Avance III spectrometer, Bruker Biospin (Fällanden, Switzerland).

Protocol

Visualization of NO-related nitrosation of DAF-FM within RBCs by laser-scanning microscopy, flow cytometry, and fluorimetry

Loading cells with DAF-FM-DA allows for visualization of NO-related nitrosation of DAF-FM within the intracellular space

using either live cell laser-scanning microscopy or flow cytometry. The former allows gaining insight into and documenting intracellular compartmentalization (e.g., to study NO formation in specific cell organelles), whereas the latter has the advantage of being able to look at larger cell numbers and the distribution of NO production across cell populations. Alternatively, changes in cell fluorescence can also be quantified by fluorimetry, although this does not allow morphological analysis or localization of the signal. Related protocols consist of loading cells with the probe by incubating them at room temperature or 37 °C for 15–60 min in the dark, washing to remove excess probe, and measuring the fluorescence activity with the technique of choice (Fig. 2). The nitrosating agent and NO donor *S*-nitrosocysteine (SNOC) may be applied as a positive control using the protocol described below [30]; for the preparation of stock solutions of other NO donors see [31]. In addition, an unloaded aliquot of cells should be kept to control for autofluorescence (Fig. 2). We recommend refraining from fixing cells to avoid interference or false positives due to the fixation process. Adherent cells might be cultured directly on coverslips [32], or in 96-well plates, and are detached by controlled proteolysis just before flow cytometric analysis.

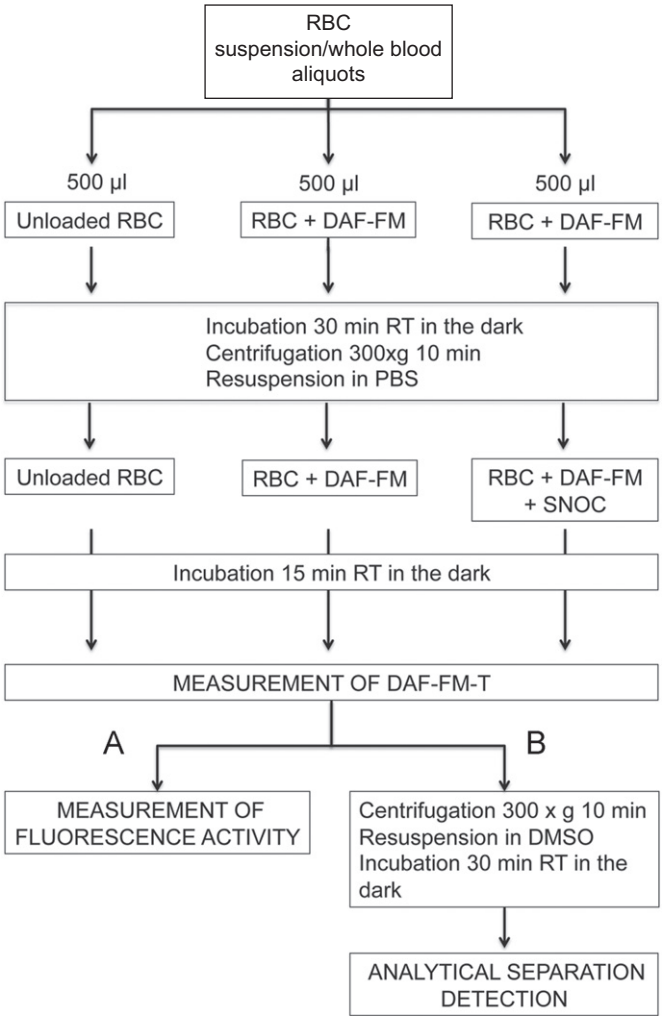

Fig. 2. Schematic representation of the DAF-FM loading protocol using red blood cells (RBCs) as an exemplary cellular system. Formation of the fluorescent product DAF-FM-T may be detected (A) by measurement of fluorescence activity using fluorescence microscopy, fluorimetry, or flow cytometry or (B) using analytical separative techniques.

Synthesis of SNOC (100 mM) [30]

(1) Dissolve 7.04 mg Cys–HCl in 192 µl double-distilled H_2O and keep on ice until use.
(2) Dissolve 2.76 mg $NaNO_2$ in 192 µl double-distilled water and keep on ice until use.
(3) Mix 192 µl Cys–HCl + 192 µl $NaNO_2$ + 8 µl 1 M HCl.
(4) Incubate 1 min at room temperature (RT); color of the solution will change to red.
(5) Equilibrate pH by adding 7–8 µl 1 M NaOH and use immediately.

Live cell laser-scanning microscopy

(1) Collect blood (1–2 ml) from the antecubital vein of healthy volunteers and add heparin (5000 U/ml).
(2) Dilute whole blood 1:10 in cold PBS and prepare 500-µl aliquots in amber Eppendorf tubes to protect DAF-FM from light.
(3) Add 1–3 µl 5 mM DAF-FM-DA (prepare by dissolving 5 µg in 20 µl dimethyl sulfoxide (DMSO) and use immediately; *do not place on ice, to avoid freezing of DMSO*). The final concentration will be 10–30 µM DAF-FM. Incubate for 30 min at RT in the dark. Keep an untreated blood aliquot as an autofluorescence control.
(4) Wash by centrifugation at 300 *g* for 10 min at 4 °C and resuspend in PBS.
(5) Add 25–100 µM SNOC and incubate for 15 min (as positive control) or leave untreated.
(6) Prepare blood smears on a glass slide with 10 µl sample.
(7) Analyze 1–2 min after preparation under a Zeiss LSM 510 confocal laser-scanning microscope (Carl Zeiss Jena GmbH) using a Zeiss Plan Neofluar 63 × /1.3 oil DIC objective and excitation

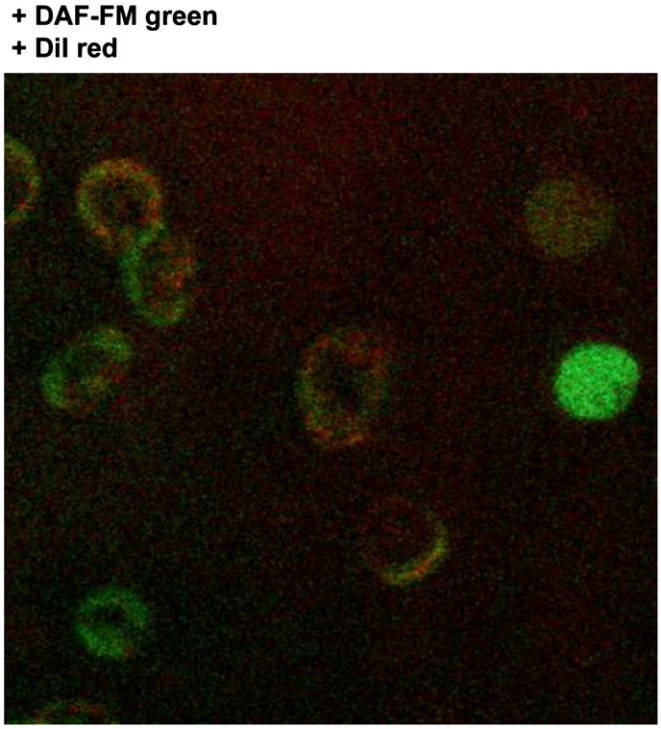

Fig. 3. Visualization of NO-related nitrosation of DAF-FM within RBCs. Micrograph of RBCs loaded with DAF-FM and the membrane stain Dil shows colocalization of the DAF-FM green fluorescence within the membrane. Representative data from 2–10 individual experiments.

488 nm with UV/488/543/633 nm beam splitter. Fluorescence should be recorded using a 540–30 nm bandpass filter.
Representative results are shown in Fig. 3.
Caveat: Exposure time should be adjusted on the SNOC-treated samples and kept constant during all measurements.

Flow cytometry

(1) Collect blood (10–12 ml) from the antecubital vein of healthy volunteers and add heparin (5000 U/ml).
(2) Dilute 1:500 in cold PBS by adding 30 µl to 15 ml PBS.
(3) Divide into 500-µl aliquots in amber Eppendorf tubes.
(4) Add 1 µl 5 mM DAF-FM-DA (dissolve 5 µg in 20 µl DMSO, and use immediately); final concentration will be 10 µM.
(5) Incubate for 30 min at RT.
(6) Wash by centrifugation at 300 g for 10 min at 4 °C.
(7) Resuspend in PBS; as a positive control add NO donors (Fig. 2).
(8) Dilute 1:3 in PBS and read fluorescence in a flow cytometer within 15 min.

The RBC population can be visualized in a double-logarithmic scatter-dot plot (foreword scatter vs side scatter). DAF-FM was excited with the 488-nm spectral line of the flow cytometer 488 nm argon laser and the signal was collected within the FITC channel (em 530 ± 30 nm). Data were collected using the flow cytometer software package (here we used DIVA 5.0; BD Bioscience).

Representative results are shown in Fig. 4.
Caveat: To standardize and ensure reliability of fluorescence acquisition, fluorescence acquisition voltage should be adjusted before each measurement according to the position of the fluorescence histogram of both the unstained control and the third fluorescence peak of standard latex beads (Rainbow beads; BD Bioscience).

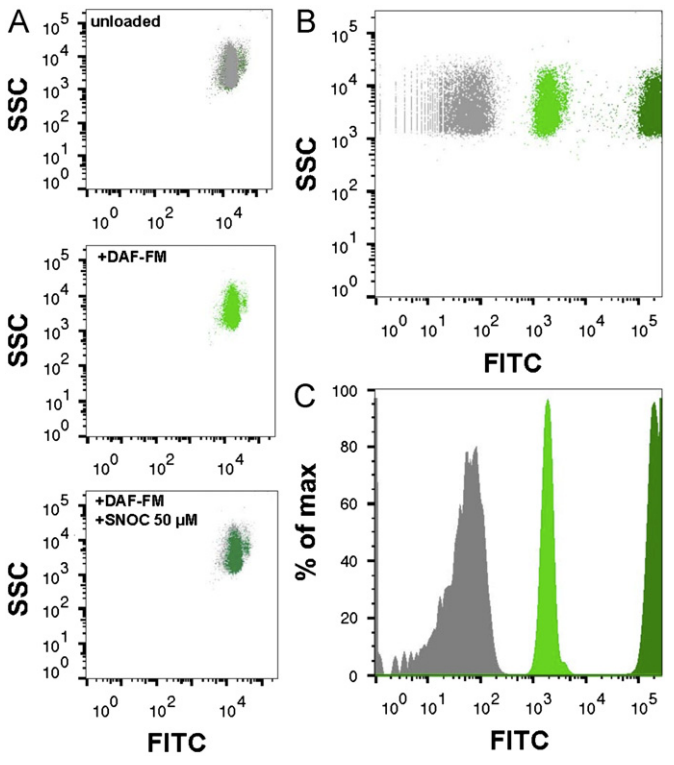

Fig. 4. Flow cytometric analysis of RBCs loaded with DAF-FM-DA. (A) Morphology of the RBC populations in a double-logarithmic scatter-dot plot. (B) Side scatter-fluorescence dot plot of unloaded cells, cells loaded with DAF-FM, and cells loaded with DAF-FM and treated with the NO donor, SNOC. (C) Fluorescence intensity distribution histogram. Representative data of $n=6$ experiments.

Fluorimetry

(1) For fluorimetric measurements follow steps 1–7 as described for flow cytometry, and refer to Table 1.
(2) Load 200 µl of samples/well in a dark 96-well plate and measure green fluorescence (ex 485, em 520).
Representative results are shown in Fig. 5.
Caveats: To ensure reproducibility of the measurements samples should be kept on ice and analyzed within 15 min. The gain should be adjusted in well mode by choosing the sample treated with SNOC (i.e., well within expected maximal intensity). Excitation time should be kept at a minimum as the fluorescence signal of fluorescein-based molecules increases on repeated exposure to light.

Analysis of DAF-FM and DAF-FM-T standards by reversed-phase HPLC and LC-MS/MS

To the best of our knowledge, no validated DAF-FM-T standard is available commercially. We prepared DAF-FM-T by reaction of DAF-FM authentic standard with SNOC (prepared as described above) and verified the purity of either stock solution by HPLC. Furthermore, we fully characterized the structure of DAF-FM by NMR and established the fragmentation patterns of both DAF-FM and DAF-FM-T by high-resolution MS (Figs. 6, 7, and 8). DAF-FM-T can be detected by HPLC with fluorescence detection, as well as by LC-MS/MS using selective-reaction monitoring (SRM) using the transition of 413.2→369.12 for DAF-FM and 424.2→380.1 for DAF-FM-T detection. Further details of the fragmentation reactions were investigated using ion trap experiments and D_2O exchange.

Preparation of DAF-FM-T

(1) Dissolve DAF-FM authentic standard (1 g) at a final concentration of 5 mM in HPLC-grade DMSO, divide into working aliquots, and keep frozen at −80 °C until use.
(2) Prepare DAF-FM-T standards by reaction of 50 µM DAF-FM with 1 mM SNOC in PBS for 30 min in the dark.

The reactants are shown in Fig. 6A.

Reversed-phase HPLC

This protocol is a modification of the method described by Rodriguez et al. for DAF-2 [22]. The method was run on an Agilent 1100 Series HPLC system (Agilent Technologies) equipped with a diode array detector and a fluorescence detector.

The column used was a Phenomenex Luna C18(2) column (4.6 µm × 250 mm; 5 µm particle size) fitted with a guard column (Phenomenex) kept constant at 25 °C.

The mobile phases were prepared as follows:

(1) Solvent A, 0.05% trifluoroacetic acid (TFA) in water;
(2) Solvent B, 0.05% TFA in acetonitrile.

The following gradient system was used with a flow rate of 1 ml/min (time, % solvent A): 0 min, 95%; 40 min, 60%; 45 min, 60%.

UV detection was set to 490 nm; fluorescence detection was conducted with an excitation wavelength of 490 nm and emission at 517 nm.

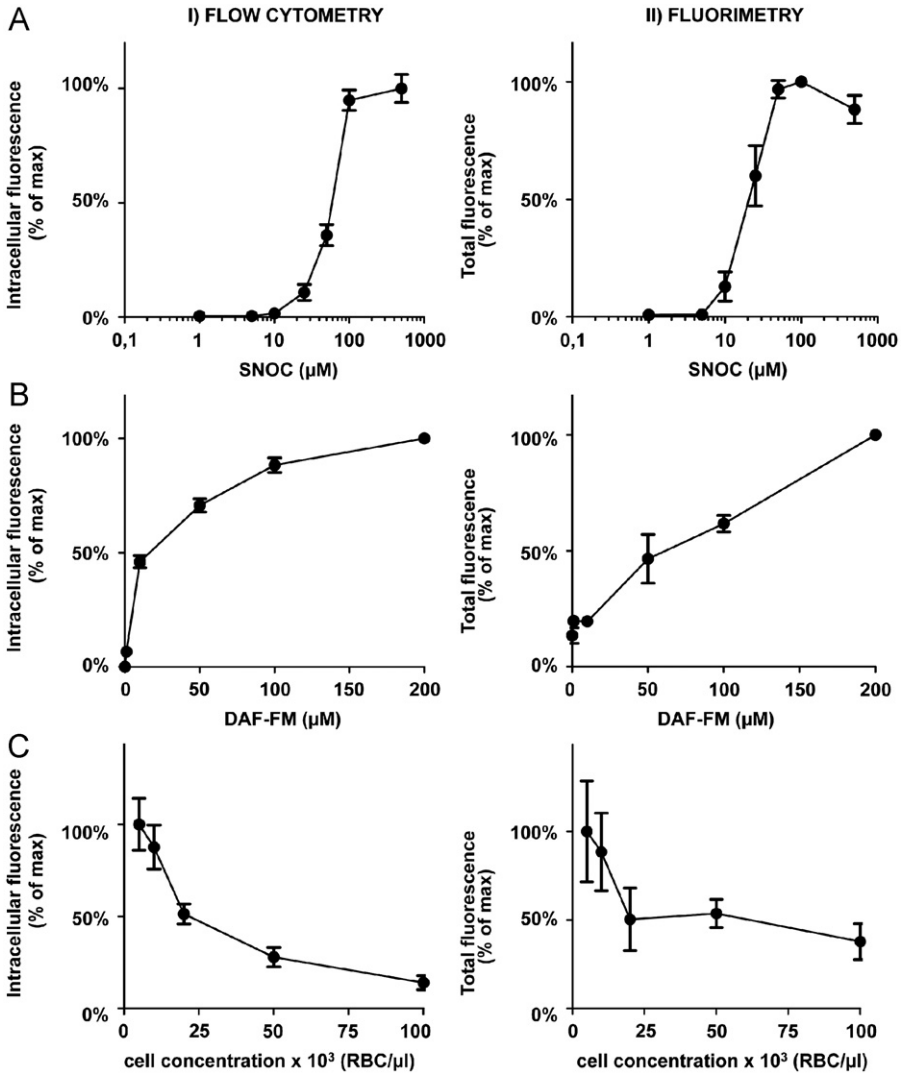

Fig. 5. Dependence of DAF-FM-associated fluorescence on NO donor and fluorescent probe concentration and on RBC number. Red cells were loaded with DAF-FM diacetate at the indicated concentrations or left untreated. Intracellular fluorescence was analyzed by flow cytometry (left) and fluorimetry (right). (A, B) Increase in fluorescence signal upon increasing concentrations of (A) SNOC and (B) DAF-FM diacetate. (C) Decrease in fluorescence signal upon increasing RBC density. Results are expressed as percentage of maximal fluorescence signal after correction for autofluorescence (means ± SEM, $n=6$).

Fig. 6B depicts representative chromatograms of DAF-FM (top) and DAF-FM-T (bottom). The peak corresponding to DAF-FM-T is marked by an arrow. Several minor fluorescent contaminants were present in the standards.

LC-MS/MS analysis

Mass spectrometric analyses were conducted using an LC-MS/MS instrument operating in positive-ionization mode. Samples were separated on a C18(2) column (50 mm × 2.1 mm). The mobile phases were prepared as follows:

(1) Solvent A, 0.1% aqueous formic acid;
(2) Solvent B, 100% methanol.

The following gradient system was used with a flow rate of 200 μl/min (time, % solvent A): 0 min, 80%; 1 min, 80%; 2.1 min, 30%; 3.1 min, 30%; 3.5 min, 80%; 5 min, 80%.

DAF-FM and DAF-FM-T were detected using SRM. The main fragmentation reaction of DAF-FM and DAF-FM-T in positive-ionization mode is the loss of CO_2.

Fig. 6C shows the pseudo-molecular ion of DAF-FM and DAF-FM-T (top row, protonated compound) and the main fragments (after loss of CO_2).

The fragmentation reactions of DAF-FM and DAF-FM-T were further investigated using high-resolution MS with an LTQ Orbitrap. Fig. 7 shows the proposed fragmentation pathway of DAF-FM and DAF-FM-T. After tautomeric rearrangement (Fig. 7, left), the primary fragmentation reaction is the loss of CO_2.

Structural analysis of DAF-FM by NMR

(1) Dissolve 1 mg DAF-FM authentic standard in 0.5 ml d_6-DMSO.
(2) Run ^{1}H NMR and ^{13}C NMR spectra of DAF-FM.

The structure and complete NMR assignments of DAF-FM (Fig. 8A) were established on the basis of various NMR spectra (^{1}H, ^{13}C, HSQC, HMBC, ^{1}H–^{1}H COSY, and NOESY), which were acquired from a solution (1 mg/0.5 ml) in d_6-DMSO at 700 MHz. The molecular formula for DAF-FM is $C_{21}H_{14}F_2N_2O_5$. However, the ^{1}H NMR spectrum shows only 8 distinct resonances (see the

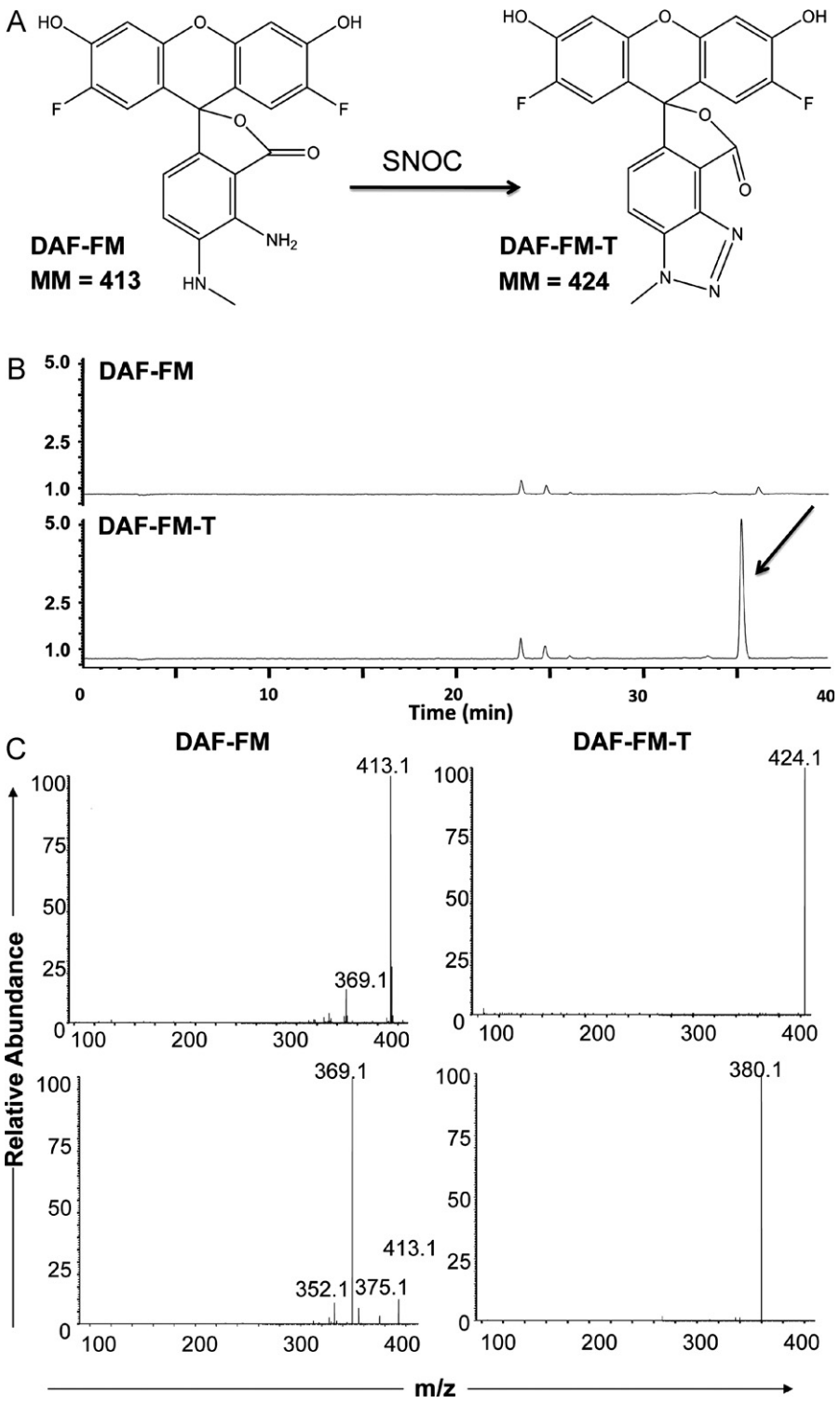

Fig. 6. Analysis of DAF-FM and DAF-FM-T by HPLC and LC-MS/MS. (A) Preparation of DAF-FM-T by reaction of DAF-FM with SNOC. (B) Representative chromatograms of DAF-FM (top) and DAF-FM-T (bottom). The peak corresponding to DAF-FM-T is marked by an arrow. (C) Representative mass spectra of DAF-FM and DAF-FM-T using LC-MS/MS; lower row represents MS/MS data of the main peak.

spectrum projected on the top in Fig. 8C; δ_H 10.69 ppm does not appear in this expansion), which is fewer than 14 peaks predicted by the molecular formula. Similarly, the ^{13}C NMR spectrum (projected on the left side of Fig. 8C; δ_C 30.1 ppm does not appear in this expansion) displays only 15 distinct resonances from a possible 21. Both ^{1}H and ^{13}C NMR spectra therefore indicate some degree of symmetry in the structure of DAF-FM. The critical resonance for elucidating the structure of DAF-FM is the quaternary carbon of the spiro-γ-lactone group at δ_C 80.9 ppm in the ^{13}C NMR spectrum. This chemical shift is consistent with an aliphatic carbon substituted by an electronegative oxygen substituent, but much less so with an aromatic carbon. It is located at the center of the molecule, as shown by four long-range connections (Fig. 8B, due to both $^{3}J_{CH}$ and $^{4}J_{CH}$)

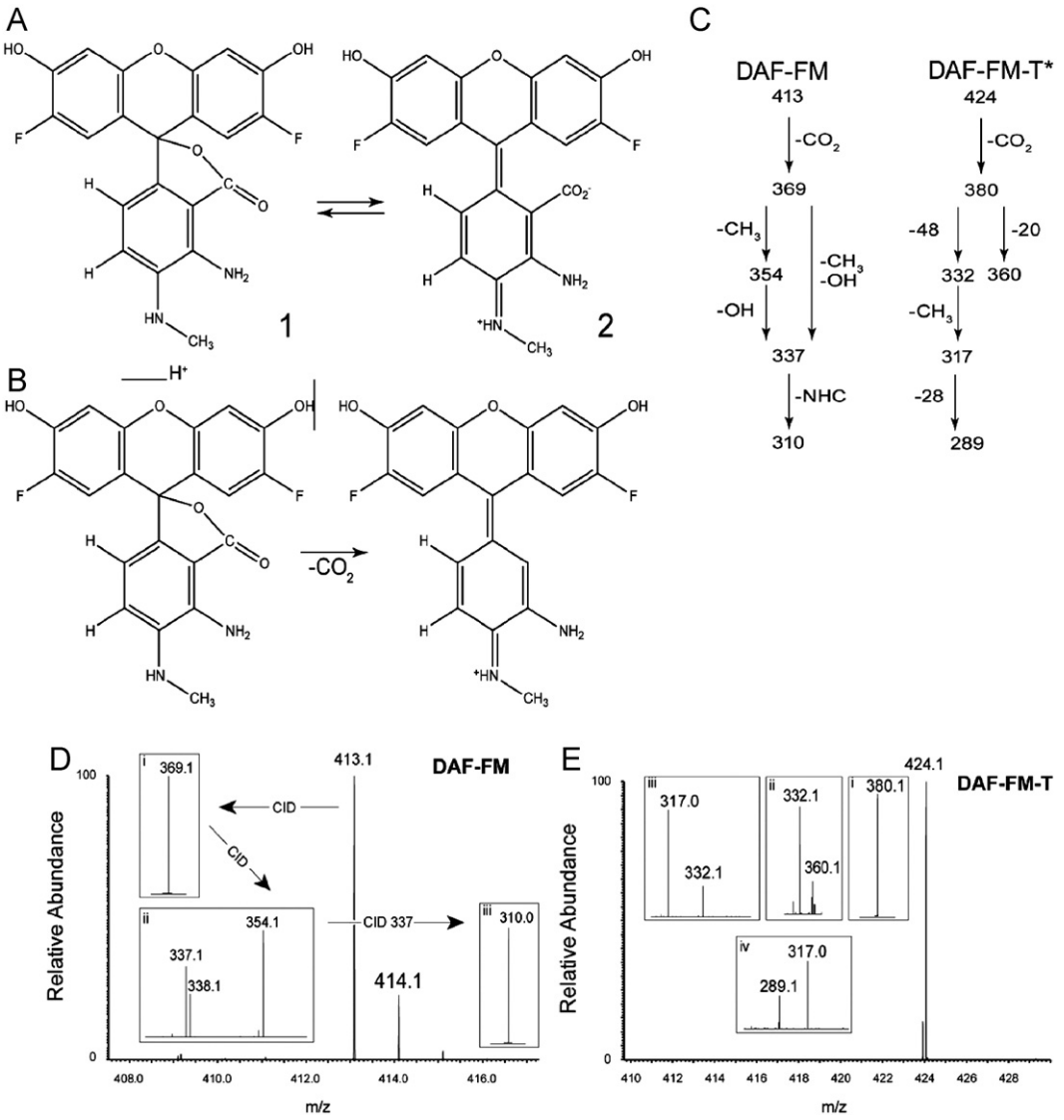

Fig. 7. Structure and fragmentation reactions of DAF-FM and DAF-FM-T. (A) Possible rearrangement of DAF-FM in solution. (B) The main fragmentation reaction of DAF-FM and DAF-FM-T in positive ionization mode is the loss of CO_2. (C) Detailed fragmentation pathway of DAF-FM and DAF-FM-T. (D, E) Fragmentation spectra of (D) DAF-FM and (E) DAF-FM-T.

in the HMBC spectrum of DAF-FM. Fig. 8B shows long-range ^{13}C–^{1}H couplings from δ_C 80.9 ppm to both hydrogens in the two (symmetrical) fluorinated aromatic rings (δ_H 6.83 and δ_H 6.48 ppm) as well as to both hydrogen atoms in the aromatic system bearing the γ-lactone moiety (δ_H 6.65 and δ_H 6.23 ppm).

HPLC and LC-MS/MS analysis of the nitrosation products of DAF-FM in Human RBCs treated with NO donors

A protocol for the detection of DAF-FM-T formation in RBCs after treatment with SNOC or the NO donor spermine/NO (Sper/NO) is provided here as an example for application of this technique to detect DAF-FM-T formation in cells (Fig. 2). As discussed above, the use of analytical separation techniques is crucial to confirm that the fluorescent signals detected by fluorimetry, laser-scanning microscopy, or flow cytometry are indeed due to intracellular nitrosation of DAF-FM (and thus originate from NO) rather than the formation of an adduct that enhances DAF-FM fluorescence in an NO-independent fashion. In addition, it offers the advantage of providing an independent semiquantitative assessment of intracellular NO production.

Preparation of Sper/NO solution

(1) dissolve Sper/NO at a concentration of 50 mM in 0.01 M NaOH, keep on ice, and use the same day.
(2) Dilute Sper/NO to desired final concentration in phosphate buffer (check that buffer strength is sufficient to bring pH to 7.4); the release of NO will begin immediately and all dilutions should be made fresh just before experimental use.

Isolation of Human RBCs

(1) Collect blood (10–12 ml) from the antecubital vein of healthy volunteers and add heparin (5000 U/ml).
(2) Transfer 10 ml of blood to a 20-ml syringe. The bottom of the syringe should be closed with a stopper. Place the syringe into a 50-ml plastic centrifugation tube and close the top with Parafilm.

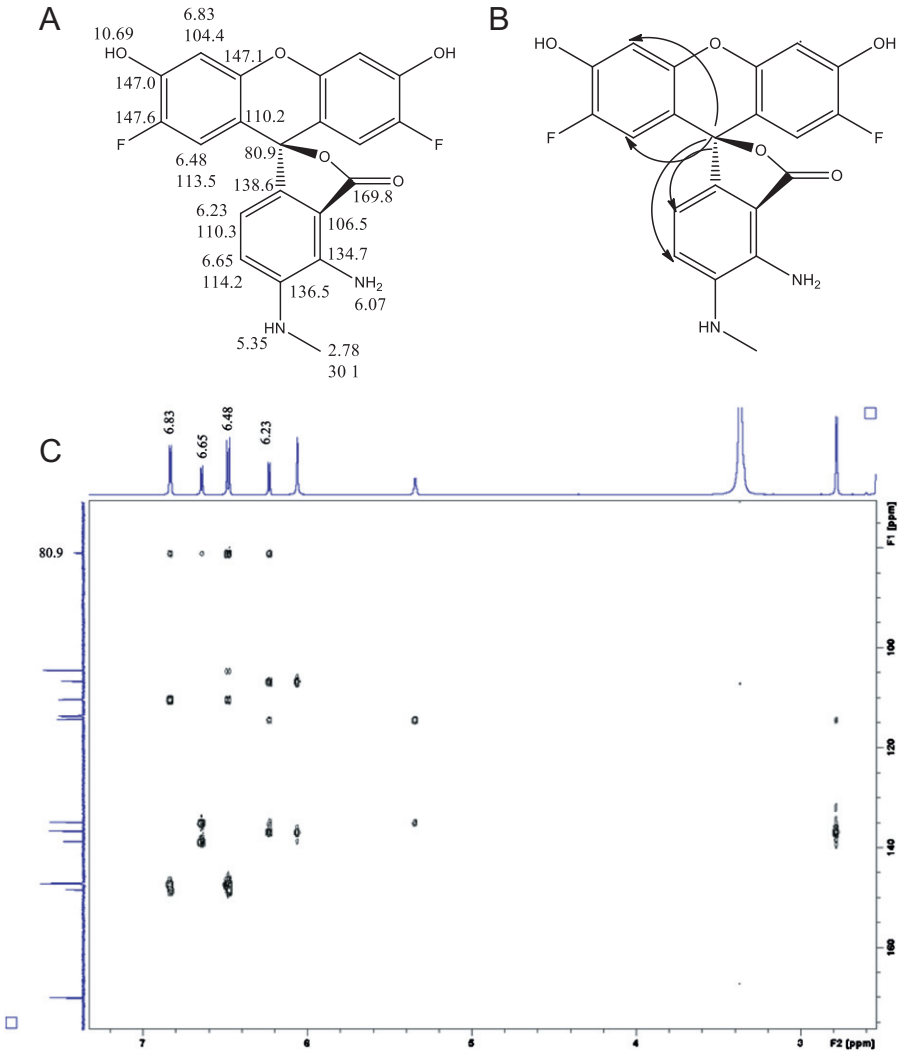

Fig. 8. Structural analysis of DAF-FM by NMR. (A) Structure and complete NMR assignments of DAF-FM. (B) Long-range ^{13}C–^{1}H couplings from δ_C 80.9 ppm to both hydrogens in the two (symmetrical) fluorinated aromatic rings (δ_H 6.83 ppm and δ_H 6.48 ppm) as well as to both hydrogens in the aromatic system, which bears the γ-lactone moiety (δ_H 6.65 ppm and δ_H 6.23 ppm). (C) HMBC spectrum with ^{13}C NMR spectrum superimposed on left side and ^{1}H NMR spectrum on top.

(3) Centrifuge the blood at 800 g for 15 min at RT. The red cell pellet can now be eluted from the bottom of the syringe.
(4) RBC concentrate should be kept on ice and used within 2 h.

Loading RBCs with DAF-FM and HPLC analysis

(1) Dilute RBC pellets 1:500 or 1:1000 in PBS (as indicated) and divide into 500-µl aliquots in amber centrifuge tubes.
(2) Add 1 µl of a 5 mM DAF-FM-DA stock solution (prepare by dissolving 5 µg in 20 µl DMSO, and use immediately); final concentration will be 10 µM DAF-FM. Incubate for 30 min at RT in the dark. Leave one sample untreated to use as matrix control (see Fig. 2).
(3) Wash by centrifugation at 300 g for 10 min at 4 °C and remove the supernatant by aspiration.
(4) Extract DAF-FM and DAF-FM-T by adding 500 µl of HPLC-grade DMSO, and incubate 30 min at RT. Keep the samples at RT from here on to avoid freezing of DMSO.
(5) Transfer the supernatant into amber Eppendorf tubes, and spin down at 13,000 g for 10 min to remove precipitates and debris.
(6) Transfer the supernatants into amber vials for HPLC and LC-MS analysis (please refer to the methods described for analysis of DAF-FM and DAF-FM-T standards).

Preparation of matrix controls

The matrix effects should be tested to document eventual changes in retention time or peak appearance and/or the presence of fluorescent contaminants.

(1) Prepare RBC lysate by diluting RBC pellets in 10 volumes of distilled water. These should be further diluted in PBS to reach a final dilution of 1:500 or 1:1000 for HPLC analysis samples.
(2) DAF-FM-T should be prepared from DAF-FM by reaction with SNOC in PBS as described above.
(3) DAF-FM-T should be diluted in the RBC lysate.

Calculations and expected results

Preliminary considerations

Subsequent loss of fluorescence of the reaction product notwithstanding, the interaction of NO (and derived nitrosated

species) with DAF-FM to form DAF-FM-T is an irreversible reaction. This suggests that increases in DAF-FM-related fluorescence intensity are cumulative in nature rather than indicative of a certain steady-state concentration of NO. Although little is known about the half-life of DAF-FM-T in cells, this compound is relatively stable in vitro. Thus, irrespective of the pitfalls described below—in particular the dependence of DAF-FM-T formation on reactive oxygen species (ROS) production (Fig. 1)—all measurements of NO using this fluorescent dye represent cumulative assessments of NO production during the chosen incubation integral.

Laser-scanning microscopy of DAF-FM-loaded RBCs

Fig. 3 depicts a typical fluorescence image of RBCs loaded with 30 μM DAF-FM-DA. To compare the fluorescence intensity of different specimens, exposure time should always be adjusted on the positive control (e.g., the SNOC-treated cells or the sample with expected maximal intensity) and kept constant during all measurements. The fluorescence intensity of individual cells can be quantified using an image-processing software package such as ImageJ (NIH) and expressed as a ratio vs DAF-FM-loaded but untreated cells. Images can be further processed for publication presentation with Adobe Photoshop CS5 (Adobe Systems GmbH, Munich, Germany) following the international guidelines for preserving image integrity [33,34].

In attempts to identify the localization of the DAF-FM-associated fluorescence within the cell membrane we co-incubated RBCs with DAF-FM-DA and the membrane tracker dye DiD (5 μg DiD/ml cell suspension). Although we found some colocalization of the green (DAF-dependent fluorescence) and the deep red (DiD) fluorescence, probe diffusion seems to limit the ability to localize NO/NO_x source(s) using this method. This may be of lesser concern if cell types other than RBCs are studied. However, both dye loading efficiency and probe distribution across cellular compartments, as well as ROS-dependent probe activation (which may differ between cell compartments), may be important confounding issues [22]. It is conceivable that particularly redox-active cell organelles such as mitochondria even support the formation of nonspecific DAF-related fluorescence by promoting dye coupling with ascorbate, for example. Thus, in our hands the technique has its limitations in terms of identifying the precise site of NO formation within the cell and may make it rather difficult to distinguish whether probe localization or reactivity accounts for a certain pattern of staining observed.

Flow cytometric and fluorimetric analysis of DAF-FM-loaded RBCs

In Fig. 4 typical data from a flow cytometric analysis of RBCs loaded with DAF-FM are presented. Data presented here were analyzed using FlowJo version 7.5.5 (TreeStar). RBCs are gated based on their size (forward light scatter) and granularity (side light scatter, SSC) in a double-logarithmic scatter-dot plot (Fig. 4A). The median fluorescence intensity (MFI) of 30,000 events within the RBC population is determined by analyzing a SSC fluorescence dot plot (Fig. 4B) or the distribution histogram (Fig. 4C). For each experiment unloaded cells served as autofluorescence control (Fig. 4, gray samples), and fluorescence activity was expressed as MFI − MFI of unloaded cells (ΔMFI).

Fig. 5 shows the change in fluorescence intensity upon variation of the concentration of SNOC (Fig. 5A), DAF-FM diacetate (Fig. 5B), or cell number (Fig. 5C). The fluorescence intensity differences obtained by flow cytometric analysis and fluorimetry are compared side by side. In fluorimetric measurements the signal is typically expressed in arbitrary units. Autofluorescence controls serve as a blank and are subtracted from the samples loaded with DAF-FM. The fluorescence activity may be expressed as percentage of maximum (as shown in Fig. 5) or as fold increase compared to samples treated with DAF-FM only.

We found that both intracellular fluorescence activity as assessed by flow cytometry (Fig. 5A, I) and total fluorescence activity as assessed by fluorimetry (Fig. 5A, II) increase with increasing SNOC concentrations in similar fashions until they reach a maximum at ~100 μM. Intracellular fluorescence increased with increasing DAF-FM concentrations in a logarithmic fashion using flow cytometry, reaching saturation around 100–200 μM DAF-FM (Fig. 5B, I), whereas total fluorescence activity linearly increased with increasing DAF-FM concentrations using fluorimetry (Fig. 5B, II). Both intracellular and total DAF-FM fluorescence intensities decreased with increasing RBC numbers (Fig. 5C). Whereas no changes in cell morphology or hemolysis were observed with these treatments at the concentrations used (which could have impeded flow cytometric analysis), a high NO/NO synthase (NOS)-independent background signal was apparent using either of these techniques, even after correction for autofluorescence, which limits the sensitivity as discussed elsewhere [22].

Detection and quantification of DAF-FM-T in RBCs by HPLC and LC-MS/MS

The structural changes associated with the preparation of DAF-FM-T from SNOC (or other NO donors) are depicted in Fig. 6A. Representative chromatograms of DAF-FM (commercial product) and DAF-FM-T (prepared by incubating DAF-FM with an excess of SNOC for 30 min at RT in the dark) standards are shown in Fig. 6B. LC-MS/MS analysis of DAF-FM and DAF-FM-T confirmed peak identities and allowed characterization of their fragmentation patterns. DAF-FM identity was additionally confirmed by ^{1}H NMR and ^{13}C NMR analysis (Fig. 8). The mass spectra of either standard, with pseudomolecular ions ($[M+H]^+$) of DAF-FM (m/z 413.1) and DAF-FM-T (m/z 424.1), are shown in Fig. 6C (top). The main fragmentation reaction for both compounds is the loss of CO_2 (m/z 44; see Fig. 7 for more details). This fragmentation reaction (413.1 → 369.1 for DAF-FM and 424.1 → 380.1 for DAF-FM-T) along with their retention times was used to detect these compounds in RBCs.

To confirm that the NO-donor-dependent fluorescent signals detected by laser-scanning microscopy, fluorimetry, and flow cytometry (Figs. 3, 4, and 5) were indeed due to intracellular nitrosation of DAF-FM to form DAF-FM-T, we analyzed the products of these reactions by HPLC and LC-MS/MS (Fig. 9). As described in detail above, RBCs were pre-loaded with DAF-FM DA and treated with SNOC or Sper/NO. Representative HPLC chromatograms are shown in Fig. 9A. The identity of an unknown peak from a cellular extract can be determined by comparing it to the retention time of the DAF-FM-T standard, and the concentration can be determined by peak integration using ChemStation (Agilent Technologies) software. A concentration-dependent increase in DAF-FM-T formation was observed in RBCs exposed to either 25–100 μM SNOC or 10–500 μM Sper/NO (Fig. 9B). No difference in retention time and/or peak area for DAF-FM-T was apparent between standards diluted in PBS and RBC lysates (to control for matrix effects). If combined with selected-reaction monitoring (i.e., multiple-reaction monitoring of the 413.1 → 369.1 and 424.1 → 380.1 transitions) by LC-MS/MS this allows both quantification and unequivocal identification of DAF-FM and DAF-FM-T in cells.

Statistical analysis

All values are reported as means ± SEM. Comparisons between groups were made using either two-tailed Student's t test or ANOVA followed by Bonferroni post hoc test for multiple comparisons. Differences were deemed significant when $p < 0.05$.

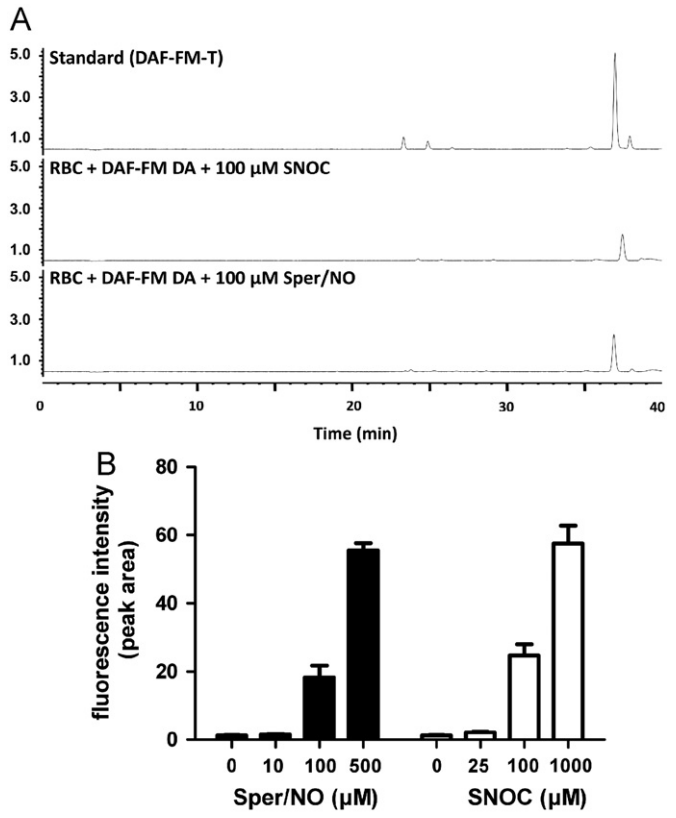

Fig. 9. Formation of DAF-FM-T and associated fluorescence increase within RBCs after addition of NO donors. (A) Representative HPLC chromatograms of DAF-FM-T standard in lysate of unlabeled RBCs (top), DAF-FM diacetate-loaded RBCs treated with SNOC (middle), or DAF-FM diacetate-loaded RBCs treated with Sper/NO (bottom). (B) Increases in DAF-FM-T formation in RBCs after treatment with NO donors as assessed by HPLC. Means ± SEM from three independent blood donors.

Statistical analyses were performed using GraphPad Prism 5.00 (GraphPad) or IBM SPSS 18.0 statistics (IBM).

Caveats

Is DAF-FM a suitable probe for measuring intracellular NO production, or Is this technique still a "triumph of Hope over reality" [35]?

Several authors have discussed the many pitfalls of using fluorescent probes for the determination of free radicals, in particular the limitations of diaminofluoresceins. Although numerous investigators are happily unaware of any such issues, others may be discouraged from experimental use altogether by this. This is unfortunate as few other techniques exist that lend themselves to assessing *intracellular* NO formation by cells. Using these probes can provide additional useful information if the following caveats are carefully considered before DAF-FM (or another diaminofluorescein) is used in biological experiments.

Probe reactivity with NO

The reaction mechanism leading to the formation of DAF-FM-T may involve nitrosative (oxidation of NO, mechanism I) or oxidative (oxidation of the probe, mechanism II) chemistry. This implies that depending on the cellular environment the probe could detect nitrosative reaction products of NO, NO itself, or both. Although testing whether the activity involves NO synthase by applying an NOS inhibitor is straightforward (see below), untangling which species accounts for the fluorescence increase can be challenging.

Presence of Interfering molecules

Oxidants and reactive oxygen species may interfere with the formation of nitrosative species from NO (according to mechanism I) and the formation of the anilinyl radical intermediate (according to mechanism II); either possibility may potentially increase the rate of formation of DAF-FM-T independent of an increase in NO formation from NOS (or another NO source). Vice versa, antioxidants can decrease it, as shown for reduced glutathione [28]. This implies that tissues/cells/conditions characterized by changes in redox-active molecules might be very difficult to compare without parallel determination of the levels of other redox parameters, including glutathione (GSH) or ROS formation.

Non-specific fluorescence products

The specificity of the DAF-FM related signal should be confirmed using NO scavengers. A typical NO scavenger used in the literature is the nitronyl nitroxide CPTIO (2-(4-carboxyphenyl)-4,4,5,5-tetramethylimidazoline-1-oxyl-3-oxide), which produces NO_2 after reaction with NO and can lead to enhanced nitrosation [36]. This may also occur with DAFs, leading to false-negative results by enhancing rather than quenching fluorescence. In our hands $Fe(DETC)_2$—which is normally used as a spin trap in ESR experiments [37]—works reasonably well as an NO scavenger, as NO is incorporated into an adduct rather than released as reactive, higher nitrogen oxide. The formation or presence of fluorescence signals unrelated to NO (adducts with, e.g., ascorbate or dehydroascorbate [27]) can be excluded by applying analytical separation techniques.

Probe accumulation and sensitivity

Effective intracellular dye accumulation may be the main reason nitrosation of DAF-FM is possible in RBCs, as demonstrated here and in vascular tissue before [22]. However, the true sensitivity of DAFs to NO donors in the cellular environment is considerably lower (in the present studies it amounted to ~25 µM Sper/NO) than in simple aqueous systems (reported to be around 5 nM) [11–14]. Probe accumulation and sensitivity should be established in your cellular system of choice, as described for RBCs here (Fig. 5).

Loading efficiency

Similar to other esterase-sensitive dyes [20], the loading efficiency of DAF-FM diacetate depends on its membrane permeability and intracellular esterase activity and thus efficiency of dye trapping. The latter may be affected by the experimental conditions (e.g., treatments) and markedly differ between cell types. Assessment of loading efficiency would require dye extraction after cell sorting, absolute determination of all DAF-FM diacetate derivates (including DAF-FM monoacetate, DAF-FM, and DAF-FM-T), and subsequent normalization to cell volume. This is rather laborious and justified only when the main objective of the study is to compare various cell types. A less accurate but much simpler approach is to use NO donors under saturating conditions, which will fully convert all intracellular DAF-FM into DAF-FM-T, and compare maximal fluorescence intensities. As long as investigators ensure that NO fluxes applied are indeed maximal for all cell types under study (requiring careful titration of the NO donor concentration) such comparison will suffice in most cases.

Photochemical reactions

Photochemical reactions may affect the probe directly by triggering nitrosative/oxidative chemistry within the cells, e.g., by inducing decomposition of preformed *S*-nitrosothiols or by UV photolysis of nitrite/nitrate. Thus, contact with light during sample preparation, incubation, and measurements should be kept to a minimum to avoid such artifacts (unless the purpose of the study is to gain information about such storage forms, of course; potential effects of added substances—to probe for specific NO-storage forms as described for $HgCl_2$ [22]—need to be verified in control experiments, e.g., in the absence of cells).

NO source

The source of NO production (e.g., endothelial NOS in RBCs) can be confirmed by pretreating cells with NOS inhibitors and/or using knockout approaches. In addition to light, thermolysis of preformed NO stores can also give rise to NO and thus increase DAF-FM-related fluorescence intensity; thus, care should be taken to carry out all experiments using reproducible temperature conditions. The diffusibility of both probe and reaction product (DAF-FM and DAF-FM-T) within the intracellular compartments and NO/NO_x, as well as the unknown kinetics of the reactions involved, can make it difficult to use DAFs for intracellular localization of an NO source.

Freezing artifacts

Introducing additional freeze/thaw cycles tends to increase autofluorescence. The reason for this is unclear, but a large (non-specific) peak at retention time 20 min is observed in the HPLC chromatogram of standards that were kept frozen. Although this will not affect the usefulness of the standards for HPLC analysis, it does affect sensitivity and potentially signal specificity.

Nitrosative chemistry of DAF-FM within RBCs

Because RBCs contain an abundance of both low-molecular-weight antioxidants, such as GSH and ascorbate, and the NO scavenger hemoglobin one wonders how DAF-FM can still detect NO and/or nitrosating species in these cells. Effective intracellular dye accumulation may be the main reason nitrosation of DAF-FM is possible in these and other cells [22]. Indeed, by analyzing the saturation curves shown in Fig. 5, we found that the probe accumulates in RBCs in a concentration- and cell number-dependent manner. However, the sensitivity of intracellular DAF-FM for extracellular added NO is rather low. In fact, HPLC and flow cytometric analyses revealed that the minimal concentration of SNOC required to significantly increase intracellular fluorescence intensity is 25 μM, and saturation of the signal under the conditions applied for flow cytometric analysis is achieved with 100 μM SNOC. At the same time, intracellular dye accumulation might strongly contribute to autofluorescence of diaminofluoresceins, e.g., because of autoxidation [22] and/or the formation of adducts with, e.g., ascorbate or dehydroascorbate [27]. Therefore, by using only fluorimetry, flow cytometry, or microscopy, the fluorescence of these secondary/nonspecific products cannot be distinguished from specific DAF-FM-T fluorescence.

For the study of DAF-FM-T formation in RBCs we characterized the structure of DAF-FM authentic standard by ^{1}H NMR and ^{13}C NMR spectrometry, as well as the fragmentation patterns of DAF-FM and DAF-FM-T. Mass spectrometric analyses of DAF-2 have been described by others previously [12,38], but to the best of our knowledge this is the first time LC-MS/MS has been used to analyze the fragmentation pattern of DAF-FM and DAF-FM-T and to confirm DAF-FM-T production in cells.

Formation of DAF-FM-T in RBCs can be induced by treatment with low micromolar concentrations of the NO donors SNOC and Sper/NO. Both NO donors are cell permeative: SNOC can be transported into RBCs by the amino acid transporters LAT-1 and LAT-2 [39,40]. However, as a nitrosothiol, SNOC not only releases NO but is also an efficient nitrosating agent. Thus, SNOC could directly nitrosate DAF-FM without the intermediacy of free NO [41]. For this reason we additionally employed the NO donor Sper/NO, which spontaneously releases NO [42]. A concentration of 100 μM Sper/NO, which translates into a constant release of 2.1–3.6 μM NO/min within the first 30 min of decomposition, also increased the formation of DAF-FM-T in RBCs with an efficacy comparable to that of SNOC.

Conclusions

Although diaminofluorescein-based fluorimetry seems to be a relatively user-friendly technique for measuring NO compared to EPR, mass spectrometry, and reductive chemiluminescence detection, in reality it is not that easy to apply. Multiple competing and confounding reactions can provide a formidable challenge to comparing different conditions (such as cell types, healthy vs diseased, etc.), which may be associated with differences in the formation of other radicals/antioxidants or oxidants at the same time. Nevertheless, and in addition to performing standard controls most investigators in this field will be familiar with, the use of analytical separation techniques capable of positively identifying the triazole product permits one to apply such probes with a fair degree of confidence for the detection of NO formation in cellular systems.

Acknowledgments

This work was supported by the Deutsche Forschungsgemeinschaft (DFG 405/5-1 and FOR809 TP7 Me1821/3-1), the Anton Betz Stiftung (26/2010), and the Susanne-Bunnenberg-Stiftung at Düsseldorf Heart Center to M.K. and the Forschungskommission of the Medical Faculty of the Heinrich Heine University of Düsseldorf (to M.C.K.). The authors thank Katharina Lysaja, Sivatharsini Thasian-Sivarajah, and Tristan Römer for indispensable assistance; Peter Heath for his support with NMR analyses; and Professor Victoria Kolb-Bachofen, Professor Dieter Häussinger, and Professor Jeremy Spencer for allowing us to use the FluostarOPTIMA, the FACS Canto II flow cytometer, and the HPLC, respectively.

References

[1] Moncada, S. Nitric oxide in the vasculature: physiology and pathophysiology. *Ann. N. Y. Acad. Sci.* **811:**67–69; 1997.
[2] Hill, B. G.; Dranka, B. P.; Bailey, S. M.; Lancaster Jr J. R.; Darley-Usmar, V. M. What part of NO don't you understand? Some answers to the cardinal questions in nitric oxide biology *J. Biol. Chem.* **285:**19699–19704; 2010.
[3] Thomas, D. D.; Ridnour, L. A.; Isenberg, J. S.; Flores-Santana, W.; Switzer, C. H.; Donzelli, S.; Hussain, P.; Vecoli, C.; Paolocci, N.; Ambs, S.; Colton, C. A.; Harris, C. C.; Roberts, D. D.; Wink, D. A. The chemical biology of nitric oxide: implications in cellular signaling. *Free Radic. Biol. Med.* **45:**18–31; 2008.
[4] Feelisch, M.; Stamler, J. *Methods in Nitric Oxide Research*. Chichester: Wiley; 1996.
[5] Feelisch, M.; Rassaf, T.; Mnaimneh, S.; Singh, N.; Bryan, N. S.; Jourd'heuil, D.; Kelm, M. Concomitant S-, N-, and heme-nitros(yl)ation in biological tissues and fluids: implications for the fate of NO in vivo. *FASEB J* **16:**1775–1785; 2002.
[6] Rassaf, T.; Bryan, N. S.; Maloney, R. E.; Specian, V.; Kelm, M.; Kalyanaraman, B.; Rodriguez, J.; Feelisch, M. NO adducts in mammalian red blood cells: too much or too little? *Nat. Med* **9:**481–482; 2003.
[7] Bryan, N. S.; Rassaf, T.; Rodriguez, J.; Feelisch, M.; Bound, NO in human red blood cells: fact or artifact? *Nitric Oxide* **10:**221–228; 2004.

[8] Giustarini, D.; Milzani, A.; Colombo, R.; le-Donne, I.; Rossi, R. Nitric oxide, S-nitrosothiols and hemoglobin: is methodology the key? *Trends Pharmacol. Sci.* **25:**311–316; 2004.
[9] Yang, B. K.; Vivas, E. X.; Reiter, C. D.; Gladwin, M. Methodologies for the sensitive and specific measurement of S-nitrosothiols, iron-nitrosyls, and nitrite in biological samples. *Free Radic. Res.* **37:**1–10; 2003.
[10] Robinson, J. K.; Bollinger, M. J.; Birks, J. W. Luminol/H_2O_2 chemiluminescence detector for the analysis of nitric oxide in exhaled breath. *Anal. Chem.* **71:**5131–5136; 1999.
[11] Kojima, H.; Sakurai, K.; Kikuchi, K.; Kawahara, S.; Kirino, Y.; Nagoshi, H.; Hirata, Y.; Nagano, T. Development of a fluorescent indicator for nitric oxide based on the fluorescein chromophore. *Chem. Pharm. Bull.* **46:**373–375; 1998.
[12] Kojima, H.; Nakatsubo, N.; Kikuchi, K.; Kawahara, S.; Kirino, Y.; Nagoshi, H.; Hirata, Y.; Nagano, T. Detection and imaging of nitric oxide with novel fluorescent indicators: diaminofluoresceins. *Anal. Chem.* **70:**2446–2453; 1998.
[13] Kojima, H.; Urano, Y.; Kikuchi, K.; Higuchi, T.; Hirata, Y.; Nagano, T. Fluorescent indicators for imaging nitric oxide production. *Angew. Chem. Int. Ed. Engl.* **38:**3209–3212; 1999.
[14] Nagano, T.; Yoshimura, T. Bioimaging of nitric oxide. *Chem. Rev.* **102:**1235–1270; 2002.
[15] Nakatsubo, N.; Kojima, H.; Kikuchi, K.; Nagoshi, H.; Hirata, Y.; Maeda, D.; Imai, Y.; Irimura, T.; Nagano, T. Direct evidence of nitric oxide production from bovine aortic endothelial cells using new fluorescence indicators: diaminofluoresceins. *FEBS Lett* **427:**263–266; 1998.
[16] Feelisch, M.; Kubitzek, D.; Werringloer, J. The oxyhemoglobin assay. In: Feelisch, M., Stamler, J., editors. *Methods in Nitric Oxide Research*. Chichester: Wiley; 1996. p. 455–478.
[17] Berliner, J. L.; Fujii, H. Magnetic resonance imaging of biological specimens by electron paramagnetic resonance of nitroxide spin labels. *Science* **227:**517–519; 1985.
[18] Villamena, F. A.; Zweier, J. L. Detection of reactive oxygen and nitrogen species by EPR spin trapping. *Antioxid. Redox Signaling* **6:**619–629; 2004.
[19] Davies, I. R.; Zhang, X. Nitric oxide selective electrodes. *Methods Enzymol.* **436:**63–95; 2008.
[20] Wardman, P. Fluorescent and luminescent probes for measurement of oxidative and nitrosative species in cells and tissues: progress, pitfalls, and prospects. *Free Radic. Biol. Med* **43:**995–1022; 2007.
[21] Kalyanaraman, B.; Darley-Usmar, V.; Davies, K. J.; Dennery, P. A.; Forman, H. J.; Grisham, M. B.; Mann, G. E.; Moore, K.; Roberts, L. J.; Ischiropoulos, H. Measuring reactive oxygen and nitrogen species with fluorescent probes: challenges and limitations. *Free Radic. Biol. Med.* **52:**1–6; 2012.
[22] Rodriguez, J.; Specian, V.; Maloney, R.; Jourd'heuil, D.; Feelisch, M. Performance of diamino fluorophores for the localization of sources and targets of nitric oxide. *Free Radic. Biol. Med.* **38:**356–368; 2005.
[23] Planchet, E.; Kaiser, W. M. Nitric oxide production in plants: facts and fictions. *Plant Signaling Behav* **1:**46–51; 2006.
[24] Hong, H.; Sun, J.; Cai, W. Multimodality imaging of nitric oxide and nitric oxide synthases. *Free Radic. Biol. Med.* **47:**684–698; 2009.
[25] Tarpey, M. M.; Wink, D. A.; Grisham, M. B. Methods for detection of reactive metabolites of oxygen and nitrogen: in vitro and in vivo considerations. *Am. J. Physiol Regul. Integr. Comp. Physiol* **286:**R431–R444; 2004.
[26] Kim, W. S.; Ye, X.; Rubakhin, S. S.; Sweedler, J. V. Measuring nitric oxide in single neurons by capillary electrophoresis with laser-induced fluorescence: use of ascorbate oxidase in diaminofluorescein measurements. *Anal. Chem.* **78:**1859–1865; 2006.
[27] Zhang, X.; Kim, W. S.; Hatcher, N.; Potgieter, K.; Moroz, L. L.; Gillette, R.; Sweedler, J. V. Interfering with nitric oxide measurements: 4,5-diaminofluorescein reacts with dehydroascorbic acid and ascorbic acid. *J. Biol. Chem.* **277:**48472–48478; 2002.
[28] Jourd'heuil, D. Increased nitric oxide-dependent nitrosylation of 4,5-diaminofluorescein by oxidants: implications for the measurement of intracellular nitric oxide. *Free Radic. Biol. Med* **33:**676–684; 2002.
[29] Hong, H.; Sun, J.; Cai, W. Multimodality imaging of nitric oxide and nitric oxide synthases. *Free Radic. Biol. Med.* **47:**684–698; 2009.
[30] Kröncke, K. D.; Kolb-Bachofen, V. Measurement of nitric oxide-mediated effects on zinc homeostasis and zinc finger transcription factors. *Methods Enzymol* **301:**126–135; 1999.
[31] Feelisch, M. The use of nitric oxide donors in pharmacological studies. *Naunyn Schmiedebergs Arch. Pharmacol* **358:**113–122; 1998.
[32] Cortese-Krott, M. M.; Munchow, M.; Pirev, E.; Hessner, F.; Bozkurt, A.; Uciechowski, P.; Pallua, N.; Kroncke, K. D.; Suschek, C. V. Silver ions induce oxidative stress and intracellular zinc release in human skin fibroblasts. *Free Radic. Biol. Med.* **47:**1570–1577; 2009.
[33] Rossner, M.; Yamada, K. M. What's in a picture? The temptation of image manipulation *J. Cell Biol.* **166:**11–15; 2004.
[34] Cromey, D. W. Avoiding twisted pixels: ethical guidelines for the appropriate use and manipulation of scientific digital images. *Sci. Eng. Ethics* **16:**639–667; 2010.
[35] Tarpey, M. M.; Fridovich, I. Methods of detection of vascular reactive species: nitric oxide, superoxide, hydrogen peroxide, and peroxynitrite. *Circ. Res.* **89:**224–236; 2001.
[36] Lakshmi, V. M.; Zenser, T. V. 2-(4-Carboxyphenyl)-4,4,5,5-tetramethylimidazoline-1-oxyl-3-oxide potentiates nitrosation of a heterocyclic amine carcinogen by nitric oxide. *Life Sci* **80:**644–649; 2007.
[37] Kleschyov, A. L.; Mollnau, H.; Oelze, M.; Meinertz, T.; Huang, Y.; Harrison, D. G.; Munzel, T. Spin trapping of vascular nitric oxide using colloid Fe(II)-diethyldithiocarbamate. *Biochem. Biophys. Res. Commun.* **275:**672–677; 2000.
[38] Ye, X.; Xie, F.; Romanova, E. V.; Rubakhin, S. S.; Sweedler, J. V. Production of nitric oxide within the Aplysia californica nervous system. *ACS Chem. Neurosci* **1:**182–193; 2010.
[39] Zhang, Y.; Hogg, N. The mechanism of transmembrane S-nitrosothiol transport. *Proc. Natl. Acad. Sci. USA* **101:**7891–7896; 2004.
[40] Satoh, S.; Kimura, T.; Toda, M.; Maekawa, M.; Ono, S.; Narita, H.; Miyazaki, H.; Murayama, T.; Nomura, Y. Involvement of L-type-like amino acid transporters in S-nitrosocysteine-stimulated noradrenaline release in the rat hippocampus. *J. Neurochem.* **69:**2197–2205; 1997.
[41] Hogg, N. Biological chemistry and clinical potential of S-nitrosothiols. *Free Radic. Biol. Med.* **28:**1478–1486; 2000.
[42] Maragos, C. M.; Morley, D.; Wink, D. A.; Dunams, T. M.; Saavedra, J. E.; Hoffman, A.; Bove, A. A.; Isaac, L.; Hrabie, J. A.; Keefer, L. K. Complexes of NO with nucleophiles as agents for the controlled biological release of nitric oxide: vasorelaxant effects. *J. Med. Chem.* **34:**3242–3247; 1991.